ISSN 1392-5113 Nonlinear Analysis: Modelling and Control, 2016, Vol. 21, No. 5, 702–715
http://dx.doi.org/10.15388/NA.2016.5.9

Glucose sensor based on nanostructured carbon electrode with immobilized PQQ-containing glucose dehydrogenase: Construction, experimental study and mathematical modeling*

Mantas Puida[a], **Jurgita Dabulytė-Bagdonavičienė**[b], **Feliksas Ivanauskas**[a], **Valdemaras Razumas**[c], **Julija Razumienė**[c], **Ieva Šakinytė**[c]

[a]Faculty of Mathematics and Informatics, Vilnius University,
Naugarduko str. 24, LT-03225 Vilnius, Lithuania
mantasp@gmail.com

[b]Department of Applied Mathematics, Kaunas University of Technology,
Studentų str. 50, LT-51368 Kaunas, Lithuania

[c]Institute of Biochemistry, Vilnius University,
Mokslininkų str. 12, LT-08662 Vilnius, Lithuania

Received: November 16, 2015 / **Revised:** June 13, 2016 / **Published online:** June 28, 2016

Abstract. Oxidized graphite (OG) has been prepared by carrying out the synthesis of graphene in the alkaline media using $K_3[Fe(CN)_6]$ as the oxidizing agent. This synthesis protocol allowed us to obtain and further to apply the OG as an effective electrode material for the reagentless enzyme electrode in which electron transfer between electrode and enzyme active site proceeds directly, without any additional mediators. Direct electron transfer in this bioelectrocatalytic system has been achieved from the active site of pyrroloquinoline quinone-containing glucose dehydrogenase (PQQ-GDH) to the nanostructurized carbon electrode surface. The numerical modeling of biosensor made possible to determine several structural and kinetic parameters of the sensor constructed. Our model of PQQ-GDH-based biosensor is built under three main assumptions. First, we assume that the electron transfer between enzyme active center and OG proceeds via the electron hopping mechanism, and therefore the rate of this reaction depends on the diffusion coefficient of an electron in OG layer. Second, enzyme is immobilized, and its diffusion coefficient is assumed to be zero. Finally, after the reaction with substrate, enzyme needs to be regenerated by the oxidized functionalities of OG.

Keywords: oxidized graphite, biosensor, PQQ-GDH, immobilized enzyme, mathematical modeling.

*This work was supported by the project "Theoretical and engineering aspects of e-service technology development and application in high-performance computing platforms" (No. VP1-3.1-ŠMM-08-K-01-010) funded by the European Social Fund.

1 Introduction

Carbonaceous materials are among those that have the greatest impact on nanotechnology. In recent decades, a large variety of carbon nanomaterials have been discovered. One of them, graphene, is in the focus of many academic and industrial scientists since 2005 after the initial publications by Novoselov, Geim, and coworkers [6, 12, 13]. Graphene represents a conceptually new class of materials that are only one atom thick and, on this basis, offers new inroads into different practical applications. Oxidation of graphite (OG) is one of the most often used [22] among other methods (sputtering [27], drawing [25], epitaxial growth [4]) of graphene preparation. This material was first prepared by Brodie [5] in 1859 by treating graphite with a mixture of $KClO_3$ and HNO_3. Later, in 1957, Hummers and Offeman developed a safer, quicker, and more efficient process, using a mixture of H_2SO_4, $NaNO_3$, and $KMnO_4$, which is still widely used [26]. Aside from the operative oxidative mechanisms, the precise chemical structure of graphite oxide (GO) has been the subject of considerable debate over the years, and even to this day no unambiguous model exists. There are many reasons for this, but the primary contributors are the complexity of the material (including sample-to-sample variability) due to its amorphous, berthollide character. While being very general, GO is a compound containing C, O, and H in variable ratios (with C:O ratio between 2.1 and 2.9 [26]). Compounds similar to GO, but with the lower content of oxygen, can be produced both electrochemically [23] and using different oxidation agents [9]. In this work, OG has been prepared by carrying out the synthesis of graphene in the alkaline media by using $K_3[Fe(CN)_6]$ as an oxidizing agent. It is likely that such oxidative treatment of graphite induces immobilized redox functionalities, and the electron transfer reaction between them proceeds via the electron hopping mechanism. This assumption is used in our current work. This synthesis protocol enabled us to obtain and apply the OG as successful electrode material for reagentless enzyme electrode in which electron transfer between electrode and enzyme active site proceeds directly, without any additional mediator of electron transfer. Direct electron transfer (DET, meaning that no redox mediator was added purposefully in the glucose solution or enzyme layer) in a bioelectrocatalytic system can be realized only by choosing the suitable enzyme, which performs DET, coupled with the appropriate electrode material, on which this enzyme can function. Using the principle of DET, it is possible to develop various bioelectrocatalytic systems useful for the investigation of enzyme-catalyzed reactions [7,8,16]. In recent years, several publications appeared where graphene nanoparticles and GO have been applied as electrode material for biosensors [10, 11, 24, 28].

It has been shown in our previous papers [17, 18] that DET can be achieved from the active site of pyrroloquinoline quinone-containing glucose dehydrogenase (PQQ-GDH) to the carbon electrode surface after the modification of carbonaceous materials. In this paper, we pursue our investigations in this area including preparation, experimental study, and mathematical characterization of the amperometric biosensor for glucose. To our knowledge, this is the first attempt to model a biosensor of this kind.

2 Experimental

Enzyme PQQ-GDH (specific activity 1717 U/mg) was purified from *Acinetobacter calcoaceticus*. The enzyme was kindly provided by the Department of Molecular Microbiology and Biotechnology (Institute of Biochemistry, Vilnius University, Lithuania). The PQQ-GDH solution of 1020 U$/$ml was prepared for the experiments. Sodium acetate, acetic acid, and $CaCl_2$ were obtained from J.T. Baker (Netherlands); $K_3[Fe(CN)_6]$, KCl, and D-glucose was purchased from Riedel-de Haën (Netherlands).

Synthesis of oxidized graphite (OG) was performed according to the method described previously [2] by treating graphite (Merck, Darmstadt, DE) with $K_3[Fe(CN)_6]$ in alkaline media. Prior to treatment, the dispersion of graphite powder (5 g) in water (20 ml) was sonicated for 10 h using VCX 130 PB sonicator (Sonycs and Materials Inc, USA). The surface area, particle and pore size of OG were analyzed using a fully automated, three-station surface area and porosity analyzer TriStar II 3020 (Micromeritics Instrument Corporation, USA). The OG was characterized by the BET surface area 10.08 m$^2/$g, the t-Plot area of micropores 0.25 m$^2/$g, the average diameter of the disc-like particles 50 nm, the average height of particles 3.5 nm, and the absorption average pore width 12.44 nm.

For designing the working electrode, OG powder was extruded by forming a tablet (diameter 2.8 mm, height 0.5 mm, weight 2.5 mg, resistance 3.2 Ω). The tablet was sealed in a Teflon tube with previously inserted copper disc of the same diameter for electrical contact. The electrode was washed with bidistilled water and dried before use. The surface of the electrode was analyzed by a scanning probe microscope Agilent 5500 AFM$/$STM (Agilent Technologies Inc, USA). The standard AFM method such as acoustic AC mode surface scanning was used for visualization of the surface morphology (Fig. 1).

The enzyme-based electrode (biosensor) was produced by mechanically attaching and fixing the membrane containing immobilized enzyme to the surface of the OG electrode. The enzyme was immobilized on a flexible support of polyvinylalcohol-coated terylene (PVA-T, Joint Institute for Nuclear Research, Dubna, Russia) by spreading of 2 μl of enzyme solution on the polymer surface (kept at $4\,^\circ$C for 1 h before use) as was described in [21]. The thickness of the PVA-T membrane with the immobilized enzyme was of ca. 14 μm (ca. 13 μm for membrane and ca. 1μm for enzyme).

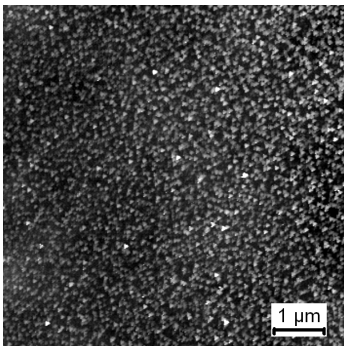

Figure 1. AFM image of OG surface.

Electrochemical measurements were performed at $25\,^{\circ}$C using electrochemical system PARSTAT 2273 (Princeton Applied Research, USA) with a conventional three-electrode system comprised of a platinum plate electrode as auxiliary, a saturated Ag/AgCl electrode as reference and PQQ-GDH-OG electrode as the working electrode. The response of enzyme electrode to the addition of the enzyme substrate D-glucose was measured under potentiostatic conditions at 0.4 V (vs. Ag/AgCl) in a stirred 0.05 M acetate buffer solution, pH 6.0, containing 10 mM Ca^{2+}.

3 Physical model of the biosensor

In order for the PQQ-GDH-OG electrode to operate properly as a glucose sensor, three reactions must proceed in this analytical system:

$$E_{ox} + S \underset{k_{-1}}{\overset{k_1}{\rightleftharpoons}} E_{ox}S \xrightarrow{k_2} E_{red} + P, \tag{1}$$

$$E_{red} + Ox \xrightarrow{k_3} E_{ox} + Red, \tag{2}$$

$$Red - 2\overline{e} \to Ox \quad \text{(electrode reaction of OG regeneration)}, \tag{3}$$

where E_{ox} is the oxidized enzyme, E_{red} is the reduced enzyme, S is the substrate D-glucose, P is the product of enzymatic reaction, $E_{ox}S$ is the complex of oxidized enzyme with substrate, Ox is the oxidized form of OG, Red is the reduced form of OG, k_1 is the rate constant of reaction between oxidized enzyme and substrate, k_{-1} is the rate constant of $E_{ox}S$ decomposition to oxidized enzyme and substrate, k_2 is the rate constant of catalytic reaction, and k_3 is the rate constant of E_{red} oxidation by OG.

A schematic view of the cross section of our biosensor system is presented in Fig. 2. The surface of OG electrode is covered with the layer of immobilized enzyme PQQ-GDH. Firstly, it is assumed that close to the OG surface, there is a very thin (1 to 2 molecular layers) zone where both OG particles and enzyme molecules are present. The enzyme layer is covered with membrane. A thin diffusion layer is formed on the outer surface of membrane when this electrode is placed in the agitated solution under investigation. Thus, six major areas can be identified (Fig. 2): Ω_1 is the area of the OG layer, Ω_2 is the area where the OG particles and enzyme molecules are mixed, Ω_3 is the area of immobilized enzyme layer, Ω_4 is the membrane, Ω_5 is the area of the D-glucose diffusion layer located between the agitated bulk solution and immobilized enzyme layer, Ω_6 is the area of the agitated substrate solution, and $d_i - d_{i-1}$ is the thickness of the corresponding areas.

In accordance with Fig. 2, reaction (1) takes place inside the areas Ω_2 and Ω_3, reaction (2) proceeds in the very thin layer Ω_2, and reaction (3) takes place in the areas Ω_1 and Ω_2.

4 Mathematical model

Our model of a PQQ-GDH-based biosensor is built under several assumptions:

1. It is assumed that reaction (3) proceeds via the electron hopping mechanism [20], and therefore the rate of this reaction depends on the diffusion coefficient of electron in the OG layer (D_e);
2. Enzyme is immobilized, and its diffusion coefficient is assumed to be zero;
3. After the reaction with substrate, enzyme needs to be regenerated by the oxidized functionalities of OG. It is assumed that this reaction takes place in the area Ω_2.

Reaction (3) is modeled as the diffusion of electrons inside the area Ω_1:

$$\frac{\partial[Ox]}{\partial t} = D_e \frac{\partial^2[Ox]}{\partial x^2}, \qquad \frac{\partial[Red]}{\partial t} = D_e \frac{\partial^2[Red]}{\partial x^2},$$

where $[Ox]$ is the concentration of oxidized functionalities of OG, and $[Red]$ is the concentration of reduced functionalities of OG.

The following initial and boundary conditions are assumed:

$$[Red](0,x) = 0, \quad [Ox](0,x) = Ox_0, \quad x \in [0; d_1],$$
$$[Red](t,0) = 0, \quad [Ox](t,0) = Ox_0, \quad t > 0,$$

where $x = 0$ corresponds to the inner surface of OG layer, $x = d_1$ corresponds to the outer surface of OG layer, and Ox_0 is the initial concentration of oxidized functionalities of OG.

The output current of the biosensor was evaluated as the gradient of reduced functionalities in OG at $x = 0$:

$$I = n_e F A D_e \frac{\partial[Red]}{\partial x}\bigg|_{x=0}, \tag{4}$$

where n_e is the number of electrons involved in redox reaction, F is the Faraday constant, and A is the surface area of the OG electrode.

As already noted, we assume that reactions (1), (2), and (3) take place in the area Ω_2. The assumption that the diffusion coefficient of enzyme equals zero implies two things: a) at the very beginning of biosensor operation, all enzyme molecules in the areas Ω_2 and Ω_3 are in the oxidized form and participate in reaction (1), but only once; b) all later operations of the biosensor are determined by the action of a very low amount of enzyme molecules in the area Ω_2, and these molecules can be reactivated there via reaction (2).

Thus, the equations describing processes taking place in the area Ω_2 are as follows:

$$\frac{\partial[Red]}{\partial t} = D_e \frac{\partial^2[Red]}{\partial x^2} + k_3[E_{red}][Ox],$$
$$\frac{\partial[Ox]}{\partial t} = D_e \frac{\partial^2[Ox]}{\partial x^2} - k_3[E_{red}][Ox],$$
$$\frac{\partial[E_{ox}]}{\partial t} = k_3[E_{red}][Ox] - k_1[S][E_{ox}] + k_{-1}[E_{ox}S],$$
$$\frac{\partial[E_{red}]}{\partial t} = -k_3[E_{red}][Ox] + k_2[E_{ox}S],$$

$$\frac{\partial[S]}{\partial t} = \frac{D_{S_2}\partial^2[S]}{\partial x^2} - k_1[S][E_{ox}] + k_{-1}[E_{ox}S],$$
$$\frac{\partial[E_{ox}S]}{\partial t} = -(k_{-1}+k_2)[E_{ox}S] + k_1[S][E_{ox}],$$

where $[E_{ox}]$ and $[E_{red}]$ are the concentrations of oxidized and reduced forms of enzyme active centers in the 1 to 2 enzyme molecular layers at the OG electrode surface (area Ω_2), $[S]$ is the substrate concentration, D_{S_2} is the diffusion coefficient of substrate in the area Ω_2, and $[E_{ox}S]$ is the concentration of the enzyme–substrate complex.

Note that from our mathematical model we excluded the equation for the accumulation of P over time since its total value does not affect the output of the biosensor.

In what follows, we define the boundary and initial conditions for the area Ω_2:

$$\begin{aligned}
&[E_{ox}](0,x) = E_0, \quad [E_{red}](0,x) = 0, && x \in [d_1;d_2],\\
&[S](0,x) = 0, \quad [E_{ox}S](0,x) = 0, && x \in [d_1;d_2],\\
&[Red](0,x) = 0, \quad [Ox](0,x) = Ox_0, && x \in [d_1;d_2],
\end{aligned}$$

$$\begin{aligned}
&D_{S_2}\frac{\partial[S]}{\partial x}(t,d_2-0) = D_{S_3}\frac{\partial[S]}{\partial x}(t,d_2+0), \quad t>0, \qquad (5)\\
&D_{S_2}\frac{\partial[S]}{\partial x}(t,d_1) = 0, \quad t>0,\\
&D_e\frac{\partial[Ox]}{\partial x}(t,d_1-0) = D_e\frac{\partial[Ox]}{\partial x}(t,d_1+0), \quad t>0,\\
&D_e\frac{\partial[Red]}{\partial x}(t,d_1-0) = D_e\frac{\partial[Red]}{\partial x}(t,d_1+0), \quad t>0,\\
&D_e\frac{\partial[Ox]}{\partial x}(t,d_2) = 0, \quad t>0,\\
&D_e\frac{\partial[Red]}{\partial x}(t,d_2) = 0, \quad t>0, \qquad (6)
\end{aligned}$$

where E_0 is the total enzyme concentration, d_2 is the interface between the areas Ω_2 and Ω_3 (Fig. 2), D_{S3} is the diffusion coefficient of the substrate in the area Ω_3.

In the area Ω_3, only reaction (1) takes place. Thus, the equations governing the processes in this area are as follows:

$$\begin{aligned}
\frac{\partial[S]}{\partial t} &= D_{S_3}\frac{\partial^2[S]}{\partial x^2} - k_1[S][E_{ox}] + k_{-1}[E_{ox}S],\\
\frac{\partial[E_{ox}]}{\partial t} &= -k_1[S][E_{ox}] + k_{-1}[E_{ox}S],\\
\frac{\partial[E_{ox}S]}{\partial t} &= -(k_{-1}+k_2)[E_{ox}S] + k_1[S][E_{ox}],\\
\frac{\partial[E_{red}]}{\partial t} &= k_2[E_{ox}S].
\end{aligned}$$

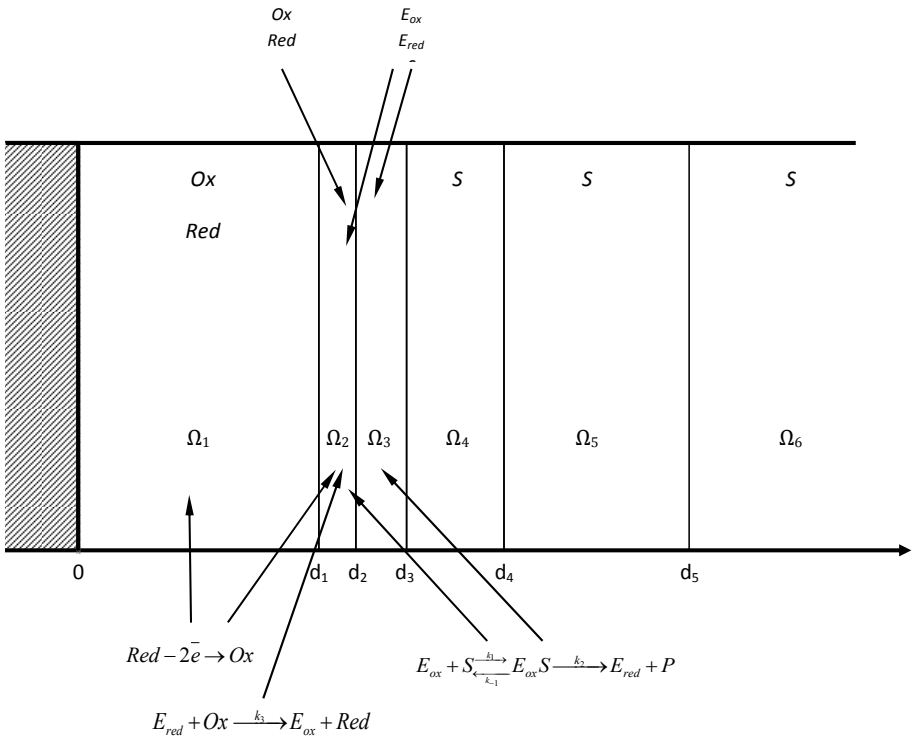

Figure 2. Reactions taking place in the specific areas of our biosensor system. Dashed area represents a disc of copper for electrical contact with OG.

The initial and boundary conditions:

$$[E_{ox}](0,x) = E_0, \quad [E_{red}](0,x) = 0, \quad x \in [d_2; d_3],$$
$$[S](0,x) = 0, \quad [E_{ox}S](0,x) = 0, \quad x \in [d_2; d_3],$$

the left side of the boundary condition for the substrate concentration S is already defined as (5),

$$D_{S_3}\frac{\partial [S]}{\partial x}(t, d_3 - 0) = D_{S_4}\frac{\partial [S]}{\partial x}(t, d_3 + 0), \quad t > 0, \tag{7}$$

where D_{S4} is the diffusion coefficient of the substrate in the area Ω_4, d_3 is the interface between the immobilized enzyme layer and outer membrane.

In the layers Ω_4 and Ω_5, only the diffusion of substrate is modeled:

$$\frac{\partial [S]}{\partial t} = D_{S_i}\frac{\partial^2 [S]}{\partial x^2}, \quad i = 4, 5.$$

The initial and boundary conditions for these processes are the following:

$$[S](0,x) = 0, \quad x \in [d_{i-1}; d_i), \quad i = 4, 5,$$

the left side of the boundary condition for the substrate concentration $[S]$ in the area Ω_4 is already defined in (7),

$$D_{S_4}\frac{\partial[S]}{\partial x}(t,d_4-0)=D_{S_5}\frac{\partial[S]}{\partial x}(t,d_4+0),\quad t>0,$$
$$[S](t,d_5)=S_0,\quad t\geqslant 0,$$

where d_4 is the outer surface of the PVA-T membrane, d_5 is the outer surface of glucose solution diffusion layer at the surface of the PVA-T membrane, D_{S_i} is the substrate diffusion coefficient in the area Ω_i, and S_0 is the substrate concentration in the bulk solution.

5 Numeric simulation results and discussion

Our numeric simulation was aimed to find a set of previously unknown parameters: the substrate diffusion coefficient D_{S_i} $(i=2,3,4)$ in the inner biosensor layers, the thickness d_2-d_1 of the OG and enzyme mixed layer, the diffusion coefficient D_e of the electron in the OG layer, that is, the parameters that shape simulated sensor response for the best fit with electrochemical experiment data. The experimental data set covering the substrate concentration range from 1.0 to 7.0 mol m^{-3} was used as a reference for fitting.

The rate constant of enzymatic reaction k_2 was primarily estimated by plotting the experimental steady-state response of biosensor against substrate concentration (Fig. 3).

It is evident from Fig. 3 that the functioning of biosensor proceeds under the kinetic control by an enzymatic reaction. Therefore, the maximum current in Fig. 3 could be estimated from $I_{S=7}=2.17$ μA by multiplying it by $(K_M+S_0)/S_0$ and assuming that $K_M=1.2$ mol m^{-3} (since $I_{\max}$ and K_M are interdependent, their final values were obtained in an iterative process of picking one of them, then calculating another one, and then adjusting the first one): $I_{\max}=2.1(1.2+7)/7=2.54$ μA. Typically, the maximum sensor response current might be expressed by the equation $I_{\max}=n_eFA\times(d_2-d_1)k_2E_0/2$ [3], though it was derived by assuming that the measured reaction

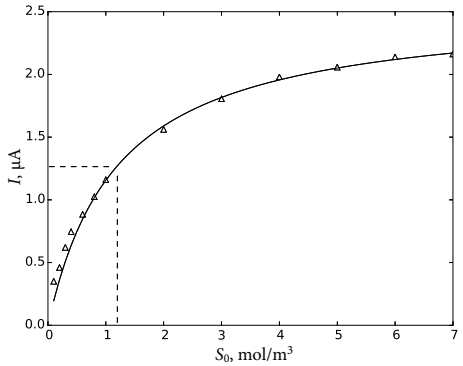

Figure 3. Dependence of experimentally measured (triangles) and simulated (solid line) steady-state current of biosensor on the substrate concentration.

product is not only consumed at the electrode surface, but also leaves the sensor active zone by diffusing into the outer solution too. In our case, the measured reaction product is Red – OG in the reduced form. These species are not leaving the active area to outer layers and is modeled with no flow boundary condition (6), which is a significant difference to the assumptions made in [3]. We derive $I_{\max}$ equation taking in to account equation (6). $I_{\max}$ is achieved at steady-state conditions, and reactions (1) proceeding in the area Ω_2 might be well approximated with Michaelis–Menten kinetics (this cannot be assumed for the area Ω_3, but since the enzyme in this area is not reactivated into the form E_{ox}, its contribution to the sensor output at the steady-state conditions is close to zero). With these assumptions in mind, we can write an equation governing the concentration of Red in the areas Ω_1 and Ω_2:

$$\frac{\partial[Red]}{\partial t} = D_e \frac{\partial^2[Red]}{\partial x^2} + \frac{V_{\max}(x)[S]}{K_M + [S]},$$

$$V_{\max}(x) = \begin{cases} k_2 E_0, & d_1 \leqslant x < d_2, \\ 0, & x < d_1. \end{cases}$$

Because reactions (1) take place only in the area Ω_2, we express this discontinuity by making $V_{\max} = 0$ in the area Ω_1. Since we assume the steady-state conditions, the change of Red concentration over time is zero:

$$\frac{\partial[Red]}{\partial t} = 0,$$

and

$$D_e \frac{\partial^2[Red]}{\partial x^2} + \frac{V_{\max}(x)[S]}{K_M + [S]} = 0$$

because $I_{\max}$ is achieved when $[S] \gg K_M$, we can eliminate $[S]$:

$$D_e \frac{\partial^2[Red]}{\partial x^2} + V_{\max}(x) = 0.$$

By integrating both sides with respect to x, we get:

$$D_e \frac{\partial[Red]}{\partial x} + \int V_{\max}(x)\,\mathrm{d}x + C = 0, \tag{8}$$

$$\int V_{\max}(x)\,\mathrm{d}x = \begin{cases} k_2 E_0 (x - d_1), & d_1 \leqslant x < d_2, \\ 0, & x < d_1. \end{cases}$$

The term C is estimated at $x = d_2$ and applying the boundary condition (6):

$$0 + \int V_{\max}(x)\,\mathrm{d}x + C = 0,$$

$$k_2 E_0 (d_2 - d_1) + C = 0, \quad C = -k_2 E_0 (d_2 - d_1).$$

To evaluate the biosensor current according to equation (4), we need to obtain the $[Red]$ gradient value at the boundary condition $x = 0$ from equation (8):

$$D_e \frac{\partial [Red]}{\partial x}(0,t) + \int V_{\max}(x)\,\mathrm{d}x\bigg|_{x=0} - k_2 E_0 (d_2 - d_1) = 0,$$

$$D_e \frac{\partial [Red]}{\partial x}(0,t) = k_2 E_0 (d_2 - d_1).$$

By substituting it into equation (4) we get

$$I_{\max} = n_e F A (d_2 - d_1) k_2 E_0. \tag{9}$$

Thus, the maximum current is twice larger compared to the case where the measured reaction product is allowed to leave the sensor surface into the outer bulk solution.

The value of k_2 was obtained from equation (9) and equals 111 s^{-1}. In turn, $k_1 = 101$ $\mathrm{m}^3\mathrm{s}^{-1}\mathrm{mol}^{-1}$ was obtained from the Michaelis constant $K_M = (k_{-1} + k_2)/k_1$.

In Table 1, we provide the values of parameters used in our further calculations.

Some parameters were fine-tuned for good match of two key features of sensor's time response, the steady-state current level and the time required to reach the steady-state. The thickness $(d_2 - d_1)$ of the enzymatic layer mixed with the OG surface particles are the parameters that mostly contribute to the absolute value of steady-state current, whereas the substrate and charge carrier diffusion coefficients mostly contribute to the period of

Table 1. Parameter values used in the mathematical model.

Parameter description	Parameter value
OG layer thickness	$d_1 = 500 \cdot 10^{-6}$ m
Thickness of OG and enzyme mixed layer	$d_2 - d_1 = 0.01 \cdot 10^{-6}$ m
Thickness of immobilized enzyme layer	$d_3 - d_2 = 10^{-6}$ m
Thickness of PVA-T membrane	$d_4 - d_3 = 13 \cdot 10^{-6}$ m
Diffusion layer thickness	$d_5 - d_4 = 30 \cdot 10^{-6}$ m
Rate constant of $E_{ox}S$ formation	$k_1 = 101$ $\mathrm{m}^3\mathrm{s}^{-1}\mathrm{mol}^{-1}$ as calculated from the value of apparent Michaelis constant in Fig. 3
Rate constant of $E_{ox}S$ backward reaction	$k_{-1} = 10$ s^{-1} [14]
Rate constant of catalytic reaction	$k_2 = 111$ s^{-1} as calculated from the maximum current value in Fig. 3
Rate constant of E_{red} oxidation by OG	$k_3 = 10^4$ $\mathrm{m}^3\mathrm{s}^{-1}\mathrm{mol}^{-1}$
Diffusion coefficient of substrate in Ω_2 area	$D_{S2} = 3.35 \cdot 10^{-10}$ $\mathrm{m}^2\mathrm{s}^{-1}$
Diffusion coefficient of substrate in Ω_3 area	$D_{S3} = 3.35 \cdot 10^{-10}$ $\mathrm{m}^2\mathrm{s}^{-1}$
Diffusion coefficient of substrate in Ω_4 area	$D_{S4} = 3.35 \cdot 10^{-10}$ $\mathrm{m}^2\mathrm{s}^{-1}$
Diffusion coefficient of substrate in Ω_5 area	$D_{S5} = 6.70 \cdot 10^{-10}$ $\mathrm{m}^2\mathrm{s}^{-1}$ [19]
Substrate concentration in bulk solution	$S_0 = [1.0; 7.0]$ mol m^{-3}
Total enzyme concentration	$E_0 = 1.93$ mol m^{-3}
Total concentration of oxidized functionalities in OG	$Ox_0 = 2$ mol m^{-3}
Number of electrons involved in redox reaction	$n_e = 2$
Faraday's constant	$F = 9.65 \cdot 10^4$ C mol^{-1}
Geometric surface area of OG electrode at the interface of areas Ω_1 and Ω_2	$A = 6.15 \cdot 10^{-6}$ m^2
Diffusion coefficient of electron in OG	$D_e = 7 \cdot 10^{-9}\mathrm{m}^2\mathrm{s}^{-1}$

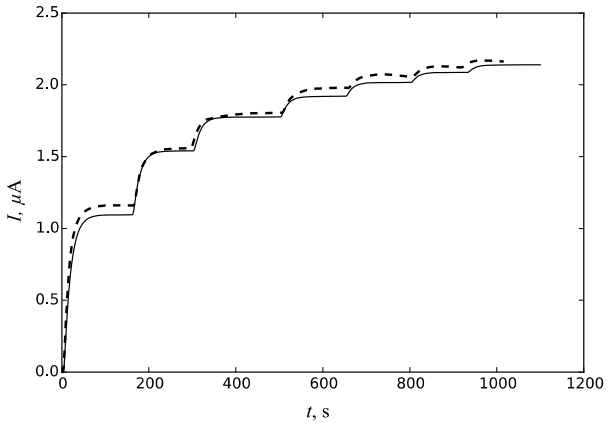

Figure 4. Biosensor's response to progressive increase of substrate concentration from 1 to 7 mol m^{-3} by 1 mol m^{-3} per step (solid line – simulated, dashed line – measured).

Table 2. Total estimated substrate concentration (TESC) in the outer solution at the specified moments of time.

Time, s	TESC, mol m^{-3}	Time, s	TESC, mol m^{-3}
0	1.0		
160	2.0	650	5.0
300	3.0	800	6.0
500	4.0	930	7.0

time needed to reach the steady-state conditions at the expense of lowering the absolute value of response current. Best-fit graph compared with the experimental measurements is presented in Fig. 4.

In Table 2, we present the sequence of substrate concentrations in the outer solution that was used for numeric simulation.

The optimal thickness value of enzyme-OG mixed layer was evaluated by using numeric simulation of $d_2 - d_1 = 0.01 \cdot 10^{-6}$ m, that is, approximately equal to the utmost dimenssion of enzyme molecule (100 Å $\times$ 50 Å $\times$ 50Å [15]). The simulation of diffusion coefficients yielded correspondingly $D_{S2} = D_{S3} = D_{S4} = 3.35 \cdot 10^{-10}$ m^{2}s^{-1}; $D_{S5} = 6.7 \cdot 10^{-10}$ m^{2}s^{-1}; $D_e = 7 \cdot 10^{-9}$m^{2}s^{-1}. The substrate diffusion coefficient D_{S_2} was chosen to yield the lowest acceptable value, which still allows a high enough response current of simulated biosensor, and also to account for how enzyme immobilization decreases the substrate diffusion rate inside the immobilized enzyme and PVA-T membrane layers.

6 Conclusions

Oxidized graphite (OG) has been synthesized and applied for the reagentless glucose biosensor design. We proposed a mathematical characterization of this amperometric biosensor based on immobilized PQQ-GDH. We proved that, when the measured reaction

product is not allowed to leave sensor's surface into the outer bulk solution, biosensor yields twice higher amperometric response when compared to the situation where it is allowed to leave sensor's surface. The numeric analysis of experiment data enables to evaluate the rate constant of forward enzymatic reaction (equation (1)) to be equal to $101\ \mathrm{m^3 s^{-1} mol^{-1}}$. The modeling of analytical system under inspection also revealed that the effective thickness of continuously reactivated enzyme layer near the OG surface plays the most important role in estimating the absolute value of the steady-state current. Diffusion of the charge carriers in OG layer largely contributes to prolonged period of time needed to reach the steady-state conditions of biosensor. The best fitted numerical simulation and experimental data have been obtained for the effective enzyme layer thickness of $d_2 - d_1 = 0.01 \cdot 10^{-6}$ m and the OG charge carrier diffusion coefficient $D_e = 7 \cdot 10^{-9}\ \mathrm{m^2 s^{-1}}$. The low diffusion coefficient of electron hopping in OG might be explained by existing structural defects in the lattice. As it is stated by Banhard et al. [1], the structural defects that may appear during preparation, deteriorate the performance of graphene-based materials. The overlap of p_z-orbitals determines the electronic properties of OG but is altered in the vicinity of structural defects. Furthermore, defects lead to a local rehybridization of σ- and π-orbitals, which again might change the electronic structure of OG.

References

1. F. Banhart, J. Kotakoski, A.V. Krasheninnikov, Structural defects in graphene, *ACS Nano*, **5**:26–41, 2011.
2. J. Barkauskas, J. Razumienė, I. Šakinytė, E. Voitechovič, Use of carbon nanomaterials for amperometric biosensors, in M. Mascini, W. Torbicz, D.G. Pijanowska (Eds.), *Micro- and Nanosystems in Biochemical Diagnosis. Principles and Application*, International Centre of Biocybernetics, 2010, pp. 28–39.
3. R. Baronas, F. Ivanauskas, J. Kulys, The influence of the enzyme membrane thickness on the response of amperometric biosensors, *Sensors*, **3**:248–262, 2003.
4. C. Berger, Z. Song, X. Li, X. Wu, N. Brown, C. Naud, D. Mayou, T. Li, J. Hass, A.N. Marchenkov, E.H. Conrad, P.N. First, W.A. de Heer, Electronic confinement and coherence in patterned epitaxial graphene, *Science*, **312**(5777):1191–1196, 2006.
5. B.C. Brodie, On the atomic weight of graphite, *Philos. Trans. R. Soc. Lond.*, **149**:249–259, 1859.
6. A.K. Geim, K.S. Novoselov, The rise of graphene, *Nat. Mater.*, **6**(3):183–91, 2007.
7. J.J. Gooding, R. Wibowo, J. Liu, W. Yang, D. Losic, S. Orbons, F.J. Mearns, J.G. Shapter, D.B. Hibbert, Protein electrochemistry using aligned carbon nanotube arrays, *J. Am. Chem. Soc.*, **125**(30):9006–7, 2003.
8. X. Kang, J. Wang, H. Wu, I.A. Aksay, J. Liu, Y. Lin, Glucose oxidase-graphene-chitosan modified electrode for direct electrochemistry and glucose sensing, *Biosens. Bioelectron.*, **25**(4):901–5, 2009.
9. L. Liu, S. Ryu, M.R. Tomasik, E. Stolyarova, N. Jung, M.S. Hybertsen, M.L. Steigerwald, L.E. Brus, G.W. Flynn, Graphene oxidation: Thickness-dependent etching and strong chemical doping, *Nano Lett.*, **8**(7):1965–70, 2008.

10. Y. Liu, D. Yu, C. Zeng, Z. Miao, L. Dai, Biocompatible graphene oxide-based glucose biosensors, *Langmuir*, **26**(9):6158–60, 2010.

11. C.-H. Lu, H.-H. Yang, C.-L. Zhu, X. Chen, G.-N. Chen, A graphene platform for sensing biomolecules, *Angew. Chem. Int. Ed.*, **48**(26):4785–7, 2009.

12. K.S. Novoselov, A.K. Geim, S.V. Morozov, D. Jiang, M.I. Katsnelson, I.V. Grigorieva, S.V. Dubonos, A.A. Firsov, Two-dimensional gas of massless dirac fermions in graphene, *Nature*, **438**(7065):197–200, 2005.

13. K.S. Novoselov, A.K. Geim, S.V. Morozov, D. Jiang, Y. Zhang, S.V. Dubonos, I.V. Grigorieva, A.A. Firsov, Electric field effect in atomically thin carbon films, *Science*, **306**(5696):666–669, 2004.

14. A.J.J. Olsthoorn, A.J. Duine, On the mechanism and specificity of soluble, quinoprotei glucose dehydro genase in the oxidation of aldose sugars, *Biochemistry*, **37**:13854–13861, 1998.

15. A. Oubrie, H.J. Rozeboom, K.H. Kalk, J.A. Duine, B.W. Dijkstra, The 1.7 Å crystal structure of the apo form of the soluble quinoprotein glucose dehydrogenase from acinetobacter calcoaceticus reveals a novel internal conserved sequence repeat, *J. Mol. Biol.*, **289**:319–333, 1999.

16. G.S. Pulcu, B.L. Elmore, D.M. Arciero, A.B. Hooper, S.J. Elliott, Direct electrochemistry of tetraheme cytochrome c_{554} from *Nitrosomonas europaea*: Redox cooperativity and gating, *J. Am. Chem. Soc.*, **129**(7):1838–1839, 2007.

17. J. Razumienė, J. Barkauskas, V. Kubilius, R. Meškys, V. Laurinavičius, Modified graphitized carbon black as transducing material for reagentless H_2O_2 and enzyme sensors, *Talanta*, **67**(4):783–90, 2005.

18. J. Razumiene, V. Gureviciene, I. Sakinyte, J. Barkauskas, K. Petrauskas, R. Baronas, Modified swcnts for reagentless glucose biosensor: Electrochemical and mathematical characterization, *Electroanalysis*, **25**:166–173, 2013.

19. A.C.F. Ribeiro, O. Ortona, S.M.N. Simões, C.I.A.V. Santos, P.M.R.A. Prazeres, A.J.M. Valente, V.M.M. Lobo, H.D. Burrows, Binary mutual diffusion coefficients of aqueous solutions of sucrose, lactose, glucose, and fructose in the temperature range from (298.15 to 328.15) k, *J. Chem. Eng. Data*, **51**:1836–1840, 2006.

20. Zh. Shuai, L. Wang, Ch. Song, *Theory of Charge Transport in Carbon Electronic Materials*, Springer Briefs in Molecular Science, Springer, Heidelberg, 2012.

21. D. Šimelevičius, K. Petrauskas, R. Baronas, J. Razumienė, Computational modeling of mediator oxidation by oxygen in an amperometric glucose biosensor, *Sensors*, **14**(2):2578–2594, 2014.

22. S. Stankovich, D.A. Dikin, G.H.B. Dommett, K.M. Kohlhaas, E.J. Zimney, E.A. Stach, R.D. Piner, S.T Nguyen, R.S. Ruoff, Graphene-based composite materials, *Nature*, **442**(7100):282–286, 2006.

23. A. Swiatkowski, M. Pakula, S. Biniak, Cyclic voltammetric studies of chemically and electrochemically generated oxygen species on activated carbons, *Electrochim. Acta*, **42**(9):1441–1447, 1997.

24. Y. Wang, Y. Shao, D.W. Matson, J. Li, Y. Lin, Nitrogen-doped graphene and its application in electrochemical biosensing, *ACS Nano*, **4**(4):1790–8, 2010.

25. J.H. Warner, M.H. Rümmeli, L. Ge, T. Gemming, B. Montanari, N.M. Harrison, B. Büchner, G.A.D. Briggs, Structural transformations in graphene studied with high spatial and temporal resolution, *Nat. Nanotechnol.*, **4**(8):500–504, 2009.

26. J. William, S. Hummers, R.E. Offeman, Preparation of graphitic oxide, *J. Am. Chem. Soc.*, **80**:1339, 1958.

27. X. Yan, J. Chen, J. Yang, Q. Xue, P. Miele, Fabrication of free-standing, electrochemically active, and biocompatible graphene oxide-polyaniline and graphene-polyaniline hybrid papers, *ACS Appl. Mater. Interfaces*, **2**(9):2521–9, 2010.

28. W. Yang, K.R. Ratinac, S.P. Ringer, P. Thordarson, J.J. Gooding, F. Braet, Carbon nanomaterials in biosensors: Should you use nanotubes or graphene?, *Angew. Chem. Int. Ed.*, **49**(12):2114–38, 2010.